



Grose, M., Black, M., Risbey, J., Uhe, P., Hope, P., Haustein, K., & Mitchell, D. M. (2018). Severe Frosts in Western Australia in September 2016. *Bulletin of the American Meteorological Society*, January 2018, S150-S154. <https://doi.org/10.1175/BAMS-D-17-0088.1>

Publisher's PDF, also known as Version of record

Link to published version (if available):
[10.1175/BAMS-D-17-0088.1](https://doi.org/10.1175/BAMS-D-17-0088.1)

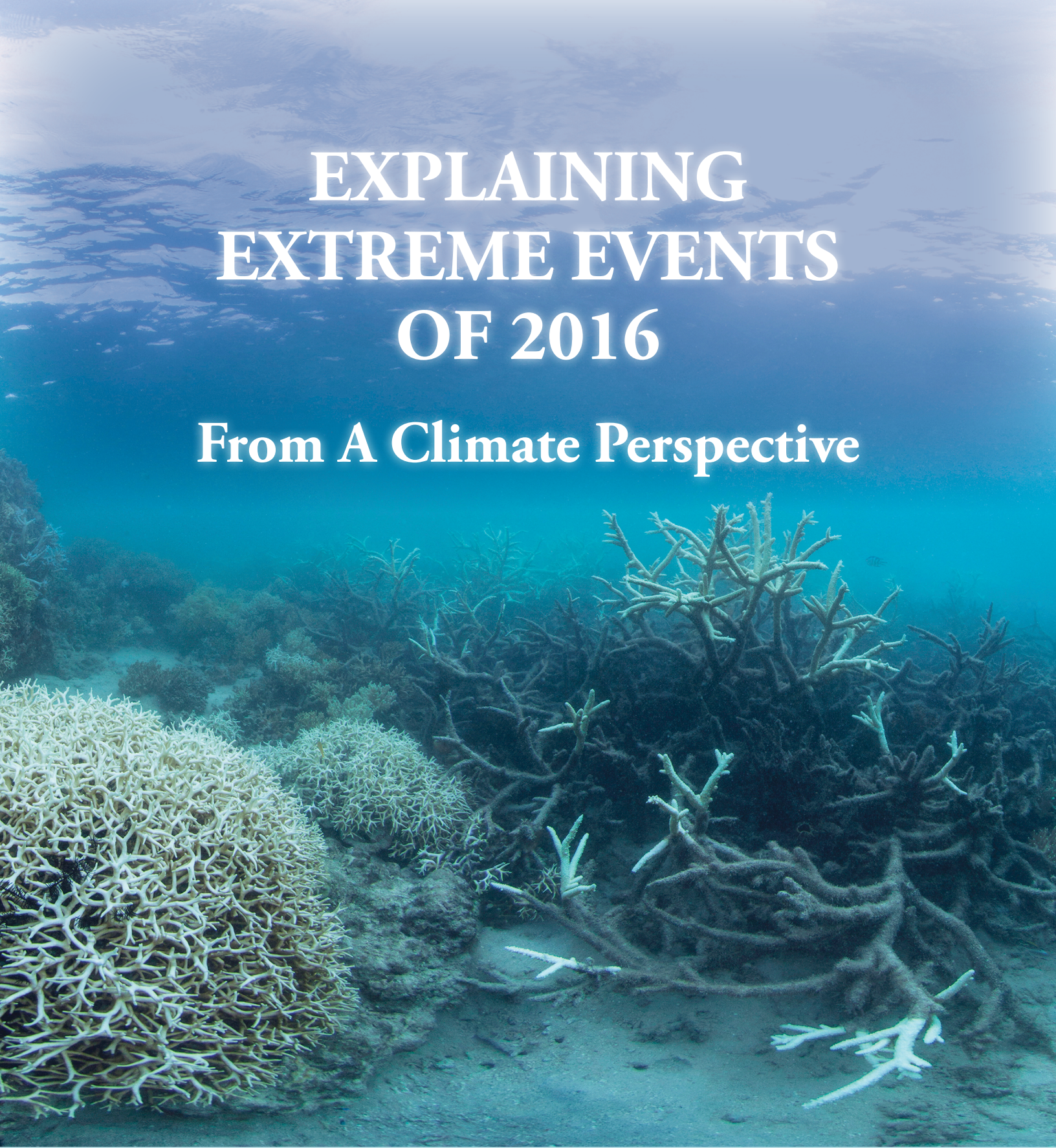
[Link to publication record in Explore Bristol Research](#)
PDF-document

This is the final published version of the article (version of record). It first appeared online via AMS at <https://journals.ametsoc.org/doi/10.1175/BAMS-D-17-0088.1> . Please refer to any applicable terms of use of the publisher.

University of Bristol - Explore Bristol Research

General rights

This document is made available in accordance with publisher policies. Please cite only the published version using the reference above. Full terms of use are available:
<http://www.bristol.ac.uk/pure/about/ebr-terms>

An underwater photograph of a coral reef. The water is a deep, clear blue. In the foreground, there are large, branching coral structures. Some of these corals are white, indicating they have lost their color due to bleaching, while others are still dark brown. The reef extends into the distance, with more coral visible under the surface.

EXPLAINING EXTREME EVENTS OF 2016

From A Climate Perspective

Special Supplement to the
Bulletin of the American Meteorological Society
Vol. 99, No. 1, January 2018

EXPLAINING EXTREME EVENTS OF 2016 FROM A CLIMATE PERSPECTIVE

Editors

Stephanie C. Herring, Nikolaos Christidis, Andrew Hoell, James P. Kossin,
Carl J. Schreck III, and Peter A. Stott

Special Supplement to the

Bulletin of the American Meteorological Society

Vol. 99, No. 1, January 2018

AMERICAN METEOROLOGICAL SOCIETY

CORRESPONDING EDITOR:

Stephanie C. Herring, PhD
NOAA National Centers for Environmental Information
325 Broadway, E/CC23, Rm 1B-131
Boulder, CO 80305-3328
E-mail: stephanie.herring@noaa.gov

COVER CREDIT:

©The Ocean Agency / XL Catlin Seaview Survey / Christophe Bailhache—A panoramic image of coral bleaching at Lizard Island on the Great Barrier Reef, captured by The Ocean Agency / XL Catlin Seaview Survey / Christophe Bailhache in March 2016.

HOW TO CITE THIS DOCUMENT

Citing the complete report:

Herring, S. C., N. Christidis, A. Hoell, J. P. Kossin, C. J. Schreck III, and P. A. Stott, Eds., 2018: Explaining Extreme Events of 2016 from a Climate Perspective. *Bull. Amer. Meteor. Soc.*, **99** (1), S1–S157.

Citing a section (example):

Quan, X.W., M. Hoerling, L. Smith, J. Perlwitz, T. Zhang, A. Hoell, K. Wolter, and J. Eischeid, 2018: Extreme California Rains During Winter 2015/16: A Change in El Niño Teleconnection? [in “Explaining Extreme Events of 2016 from a Climate Perspective”]. *Bull. Amer. Meteor. Soc.*, **99** (1), S54–S59, doi:10.1175/BAMS-D-17-0118.1.

EDITORIAL AND PRODUCTION TEAM

Riddle, Deborah B., Lead Graphics Production, NOAA/NESDIS National Centers for Environmental Information, Asheville, NC

Love-Brotak, S. Elizabeth, Graphics Support, NOAA/NESDIS National Centers for Environmental Information, Asheville, NC

Veasey, Sara W., Visual Communications Team Lead, NOAA/NESDIS National Centers for Environmental Information, Asheville, NC

Fulford, Jennifer, Editorial Support, Telesolv Consulting LLC, NOAA/NESDIS National Centers for Environmental Information, Asheville, NC

Griffin, Jessica, Graphics Support, Cooperative Institute for Climate and Satellites-NC, North Carolina State University, Asheville, NC

Misch, Deborah J., Graphics Support, Telesolv Consulting LLC, NOAA/NESDIS National Centers for Environmental Information, Asheville, NC

Osborne, Susan, Editorial Support, Telesolv Consulting LLC, NOAA/NESDIS National Centers for Environmental Information, Asheville, NC

Sprain, Mara, Editorial Support, LAC Group, NOAA/NESDIS National Centers for Environmental Information, Asheville, NC

Young, Teresa, Graphics Support, Telesolv Consulting LLC, NOAA/NESDIS National Centers for Environmental Information, Asheville, NC

TABLE OF CONTENTS

Abstract.....	ii
1. Introduction to Explaining Extreme Events of 2016 from a Climate Perspective	1
2. Explaining Extreme Ocean Conditions Impacting Living Marine Resources	7
3. CMIP5 Model-based Assessment of Anthropogenic Influence on Record Global Warmth During 2016.....	11
4. The Extreme 2015/16 El Niño, in the Context of Historical Climate Variability and Change	16
5. Ecological Impacts of the 2015/16 El Niño in the Central Equatorial Pacific	21
6. Forcing of Multiyear Extreme Ocean Temperatures that Impacted California Current Living Marine Resources in 2016	27
7. CMIP5 Model-based Assessment of Anthropogenic Influence on Highly Anomalous Arctic Warmth During November–December 2016.....	34
8. The High Latitude Marine Heat Wave of 2016 and Its Impacts on Alaska.....	39
9. Anthropogenic and Natural Influences on Record 2016 Marine Heat waves.....	44
10. Extreme California Rains During Winter 2015/16: A Change in El Niño Teleconnection?.....	49
11. Was the January 2016 Mid-Atlantic Snowstorm "Jonas" Symptomatic of Climate Change?.....	54
12. Anthropogenic Forcings and Associated Changes in Fire Risk in Western North America and Australia During 2015/16.....	60
13. A Multimethod Attribution Analysis of the Prolonged Northeast Brazil Hydrometeorological Drought (2012–16).....	65
14. Attribution of Wintertime Anticyclonic Stagnation Contributing to Air Pollution in Western Europe.....	70
15. Analysis of the Exceptionally Warm December 2015 in France Using Flow Analogues.....	76
16. Warm Winter, Wet Spring, and an Extreme Response in Ecosystem Functioning on the Iberian Peninsula	80
17. Anthropogenic Intensification of Southern African Flash Droughts as Exemplified by the 2015/16 Season	86
18. Anthropogenic Enhancement of Moderate-to-Strong El Niño Events Likely Contributed to Drought and Poor Harvests in Southern Africa During 2016	91
19. Climate Change Increased the Likelihood of the 2016 Heat Extremes in Asia	97
20. Extreme Rainfall (R20mm, RX5day) in Yangtze–Huai, China, in June–July 2016: The Role of ENSO and Anthropogenic Climate Change.....	102
21. Attribution of the July 2016 Extreme Precipitation Event Over China’s Wuhang	107
22. Do Climate Change and El Niño Increase Likelihood of Yangtze River Extreme Rainfall?.....	113
23. Human Influence on the Record-breaking Cold Event in January of 2016 in Eastern China.....	118
24. Anthropogenic Influence on the Eastern China 2016 Super Cold Surge.....	123
25. The Hot and Dry April of 2016 in Thailand.....	128
26. The Effect of Increasing CO ₂ on the Extreme September 2016 Rainfall Across Southeastern Australia.....	133
27. Natural Variability Not Climate Change Drove the Record Wet Winter in Southeast Australia	139
28. A Multifactor Risk Analysis of the Record 2016 Great Barrier Reef Bleaching	144
29. Severe Frosts in Western Australia in September 2016.....	150
30. Future Challenges in Event Attribution Methodologies.....	155

This sixth edition of explaining extreme events of the previous year (2016) from a climate perspective is the first of these reports to find that some extreme events were not possible in a preindustrial climate. The events were the 2016 record global heat, the heat across Asia, as well as a marine heat wave off the coast of Alaska. While these results are novel, they were not unexpected. Climate attribution scientists have been predicting that eventually the influence of human-caused climate change would become sufficiently strong as to push events beyond the bounds of natural variability alone. It was also predicted that we would first observe this phenomenon for heat events where the climate change influence is most pronounced. Additional retrospective analysis will reveal if, in fact, these are the first events of their kind or were simply some of the first to be discovered.

Last year, the editors emphasized the need for additional papers in the area of “impacts attribution” that investigate whether climate change’s influence on the extreme event can subsequently be directly tied to a change in risk of the socio-economic or environmental impacts. Several papers in this year’s report address this challenge, including Great Barrier Reef bleaching, living marine resources in the Pacific, and ecosystem productivity on the Iberian Peninsula. This is an increase over the number of impact attribution papers than in the past, and are hopefully a sign that research in this area will continue to expand in the future.

Other extreme weather event types in this year’s edition include ocean heat waves, forest fires, snow storms, and frost, as well as heavy precipitation, drought, and extreme heat and cold events over land. There were

a number of marine heat waves examined in this year’s report, and all but one found a role for climate change in increasing the severity of the events. While human-caused climate change caused China’s cold winter to be less likely, it did not influence U.S. storm Jonas which hit the mid-Atlantic in winter 2016.

As in past years, the papers submitted to this report are selected prior to knowing the final results of whether human-caused climate change influenced the event. The editors have and will continue to support the publication of papers that find no role for human-caused climate change because of their scientific value in both assessing attribution methodologies and in enhancing our understanding of how climate change is, and is not, impacting extremes. In this report, twenty-one of the twenty-seven papers in this edition identified climate change as a significant driver of an event, while six did not. Of the 131 papers now examined in this report over the last six years, approximately 65% have identified a role for climate change, while about 35% have not found an appreciable effect.

Looking ahead, we hope to continue to see improvements in how we assess the influence of human-induced climate change on extremes and the continued inclusion of stakeholder needs to inform the growth of the field and how the results can be applied in decision making. While it represents a considerable challenge to provide robust results that are clearly communicated for stakeholders to use as part of their decision-making processes, these annual reports are increasingly showing their potential to help meet such growing needs.

29. SEVERE FROSTS IN WESTERN AUSTRALIA IN SEPTEMBER 2016

MICHAEL R. GROSE, MITCHELL BLACK, JAMES S. RISBEY, PETER UHE, PANDORA K. HOPE,
KARSTEN HAUSTEIN, AND DANN MITCHELL

Human influence may have enhanced the circulation pattern that drives cold outbreaks and frost risk over southwest Western Australia in September 2016, but larger thermodynamic changes may have still made these events less likely.

Introduction. The wheat belt of southwest Western Australia (SWWA) experienced several severe frosts just before harvest in September 2016, leading to a loss of one million tonnes of grain crops (GIWA 2016). Using the Jones et al. (2009) gridded observation dataset, there were 18 frost-risk nights ($T_{\min} < 2^{\circ}\text{C}$) somewhere in the grain belt through the month and the September frost area and frequency was extensive (Fig. 29.1a), the highest since 1956. The highest count at any grid cell was 13 frost-risk nights, with 9 severe frost-risk nights ($T_{\min} < 0^{\circ}\text{C}$). Many places saw the highest number of September frost nights since reliable records began in 1910, with most of the region in the top five years (Fig. 29.1b). SWWA also saw below-average rainfall and humidity, southerly monthly wind anomalies, and cool sea surface temperatures (SSTs) immediately adjacent to SWWA in September. There were weak La Niña and negative Indian Ocean Dipole conditions during September.

The effect of human influence on cold extremes is the net result of two influences: rising temperatures of the climate mean state and forced changes to circulation. The SWWA region has warmed by around 1°C since 1910, suggesting a reduction in frost risk (BOM and CSIRO 2016). However, greenhouse gas forcing may drive an increase in the frequency or intensity of

some cold extremes through an effect on circulation features, offsetting or countering the effect of the rising mean temperature. There is a hypothesized link between climate change and a shift in circulation linked to increased cold extremes in the northern hemisphere (e.g., Cohen et al. 2014; Zhang et al. 2016; Mann et al. 2017). In some regions of southern Australia, frost frequency and the length of the frost season has been increasing despite an increase in mean temperature in all seasons (Crimp et al. 2016). The driver of the increase is not completely clear but may be linked to circulation changes forced by greenhouse gases. An increase in pressure around the midlatitudes has been attributed to greenhouse gases (e.g., Gillett et al. 2013). This trend has included an intensification of the subtropical ridge, but the ridge has only a weak connection to frost risk through promoting clear skies. The link to frosts may be more a function of the particular mean sea level pressure (MSLP) anomalies.

Cold outbreaks and frost risk in SWWA are often associated with a positive MSLP anomaly over the Indian Ocean west of Australia and a negative MSLP anomaly across southern and southeastern Australia, advecting cold air from the south of Australia over SWWA (Ashcroft et al. 2009; Pook et al. 2011). Numerous days in September 2016 showed this MSLP signature, expressed as slow moving blocking highs in the Indian Ocean sector at $\sim 40^{\circ}\text{S}$. An important question, therefore, is whether this circulation anomaly was made more likely due to greenhouse forcing. The peak of blocking in the southeast Australian sector in winter is projected to weaken and move eastward (Grose et al. 2017). However, blocking in the Indian Ocean sector in spring may have a different response. Indeed, exceptionally high MSLP south of Australia in August 2014 was more likely due to human influence (Grose et al. 2015), and this was linked to blocking highs.

AFFILIATIONS: GROSE AND RISBE—CSIRO Ocean and Atmosphere, Hobart, Tasmania, Australia; BLACK—ARC Centre of Excellence for Climate System Science and University of Melbourne, Melbourne, Victoria, Australia; UHE—Environmental Change Institute, University of Oxford, and Oxford e-Research Centre, University of Oxford, Oxford, United Kingdom; HOPE—Bureau of Meteorology, Melbourne, Victoria, Australia; HAUSTEIN—Environmental Change Institute, University of Oxford, Oxford, United Kingdom; MITCHELL—Environmental Change Institute, University of Oxford, Oxford, and School of Geographical Sciences, University of Bristol, Bristol, United Kingdom

DOI:10.1175/BAMS-D-17-0088.1

A supplement to this article is available online (10.1175/BAMS-D-17-0088.2)

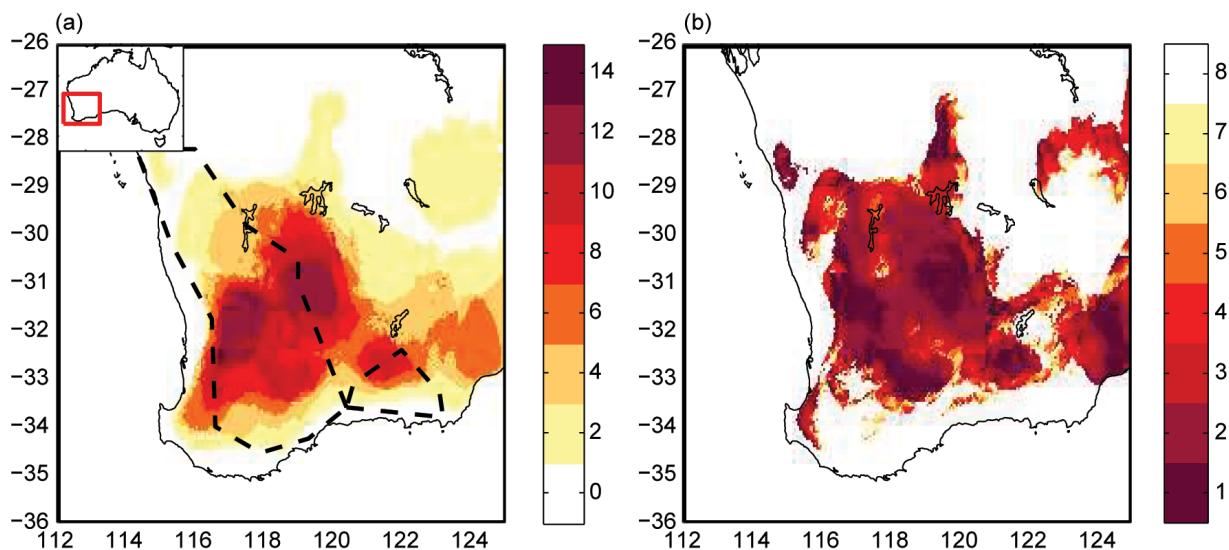


FIG. 29.1. (a) Frost risk nights ($T_{\min} < 2^{\circ}\text{C}$) in Sep 2016 in the AWAP gridded dataset [number of nights (out of 30)], dashed line shows rough outline of SWWA wheat belt, inset shows the location of SWWA within Australia; (b) rank of Sep 2016 frost frequency within the 1910–2016 record.

While there have been studies on trends in frosts (e.g., Crimp et al. 2016), there have been no previous studies showing a link between a particular cold extreme event or frosts and human influence. Here we examine the SWWA September frosts and whether the MSLP and blocking may have offset or countered the mean warming effects.

Methods. We examined daily minimum temperature, MSLP, the blocking index and blocking events using the Tibaldi and Molteni (1990) index in ERA-Interim reanalysis (Dee et al. 2011), the global *weather@home* modeling system version 2 (Guilod et al. 2017) and the seasonal climate forecasting system Predictive Ocean Atmosphere Model for Australia (POAMA; Hope et al. 2016; Wang et al. 2016).

We examined the difference in circulation between 165 *weather@home* simulations of September 2016 with observed forcings (Factual simulations) and 287 *weather@home* simulations of a counterfactual September 2016 without human influence (Counterfactual simulations). Ensembles were generated by running the model with perturbed atmospheric initial conditions. The Factual simulations used observed SSTs and sea ice, as well as present-day atmospheric composition (long-lived greenhouse gases, ozone, and aerosols). The Counterfactual simulations used SSTs modified to remove different estimates of the warming attributable to anthropogenic forcing and preindustrial atmospheric composition. Estimates of the SST changes due to anthropogenic forcing were separately calculated using twelve CMIP5 models

(Taylor et al. 2012) and the mean of those models (Table ES29.1). These patterns are the difference between the SSTs in the CMIP5 models' historical and historicalNAT simulations and are not the same as warming in observed datasets. The number of simulations from each model did not yield a sufficient sample size, so we examine 287 Counterfactual simulations as a group. Climatologies of 1986–2015 for Factual and Counterfactual were also examined.

POAMA forecasts were initialized after the first week of September 2016 and run for the last 3-week period of the month, see Hope et al. (2018) for more detail. Two 44-member ensemble forecasts were made—one under current levels of carbon dioxide (Factual) and another that removes the influence of the last 55 years of carbon dioxide increase on the ocean warming, atmospheric radiation balance, and land (Counterfactual; see Wang et al. 2016). Note that the POAMA system accounts for changes in greenhouse gases; it does not account for changes in ozone or aerosol. Climatologies for the years 2000–14 under both high and low levels of carbon dioxide were also examined.

The seasonal means of *weather@home* geopotential height in the region are similar to reanalysis (Guilod et al. 2017), and some midlatitude circulation features relevant to extreme temperatures in the northern hemisphere are well reproduced but with too many short-lived blocking events (Mitchell et al. 2017). The Tibaldi and Molteni blocking index and frequency of detections near SWWA is fairly similar between *weather@home* and ERA-Interim

(Fig. ES29.1). POAMA is similar to reanalysis in terms of broad circulation (Wang et al. 2016), but underestimates the strength and frequency of blocking (Marshall et al. 2014).

Results. Examining the observed circulation component of the frost risk, we see enhanced September MSLP west of SWWA and a low anomaly in southeast Australia and a southerly 850-hPa wind anomaly of 2.3 m s^{-1} at the south coast of SWWA (Fig. 29.2a), which is consistent with the typical cold outbreak events (Ashcroft et al. 2009). The monthly MSLP anomaly reflects the presence of persistent highs adjacent to SWWA on many days (not shown), particularly through the middle of the month. In

daily data, MSLP was enhanced at 70° – 110°E by up to 18 hPa and/or diminished in the region 110° – 140°E with southerly wind anomalies over SWWA on many of the days.

Monthly *weather@home* MSLP was higher in Factual compared to Counterfactual west of SWWA (Fig. 29.2b), creating a higher monthly southerly 850 hPa wind anomaly at the south coast of SWWA (Counterfactual mean was 2.1 m s^{-1} ; Factual mean was 2.4 m s^{-1} , giving an enhancement of $+0.3 \text{ m s}^{-1}$). Even though these wind anomalies do not penetrate inland, they suggest greater transport of cold air into the broader region and an enhancement of the circulation anomaly favoring frost nights in SWWA. The negative MSLP anomaly in southeast Australia was

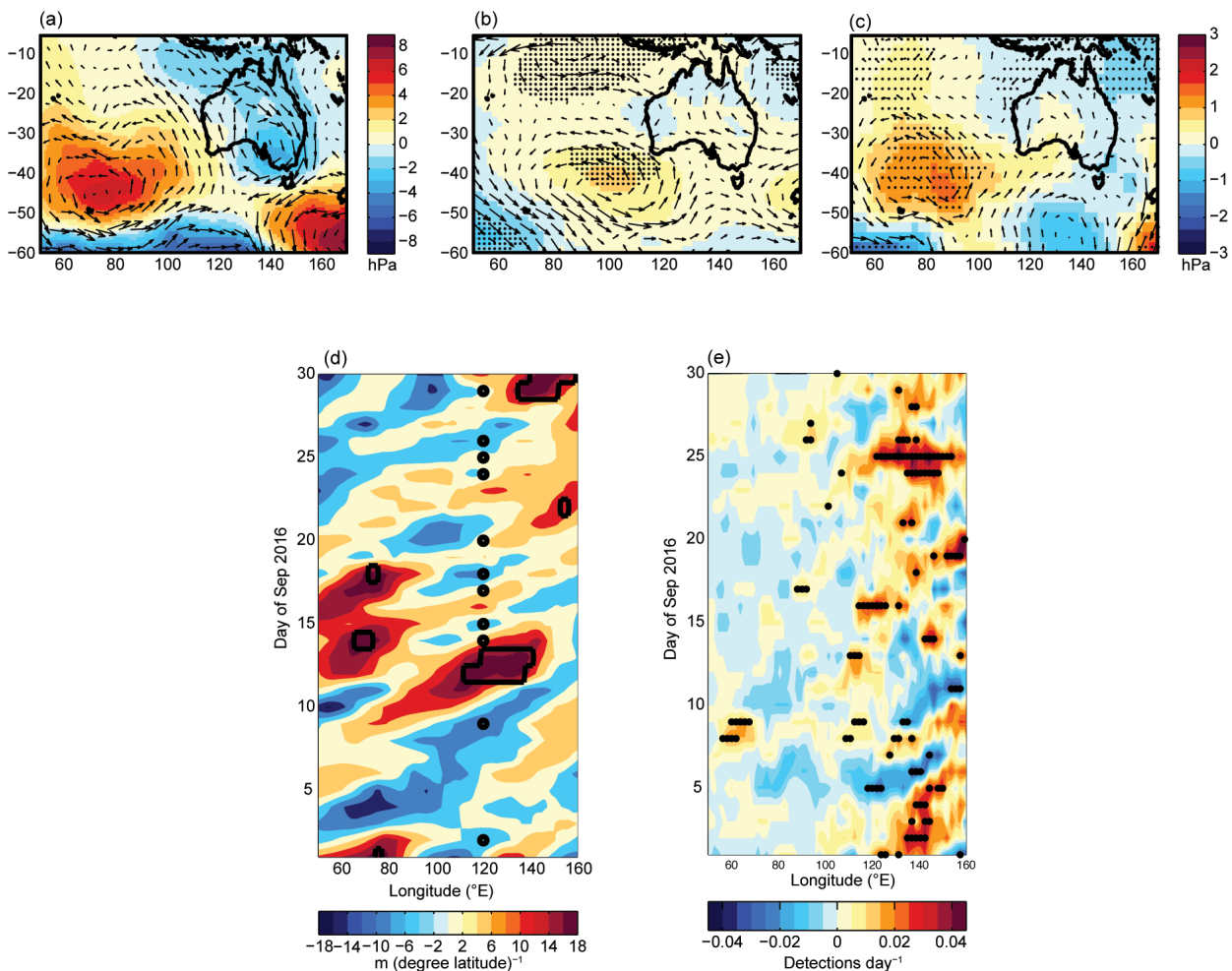


FIG. 29.2. MSLP, wind, and blocking in ERAint and models in Sep 2016; (a) ERAint monthly MSLP anomaly from 1979–2016 mean, arrows indicate the 850-hPa wind anomaly; (b) Factual–Counterfactual MSLP difference in *weather@home* mean, stippling shows where the difference is significant at the 10% level (t test), arrows show the Factual–Counterfactual 850-hPa wind difference; (c) as in (b) in POAMA; (d) ERA-Interim daily blocking index anomaly from 1979–2016 mean, black outlines indicate detected blocking events (no minimum event length threshold applied) and black circles indicate frost events at the approximate longitude of SWWA; (e) Factual–Counterfactual Blocking mean blocking event detections (detections day^{-1}) in *weather@home*, stippling shows where the difference is significant at the 10% level (t test).

not enhanced in Factual compared to Counterfactual (Fig. 29.2b). In daily data, there was higher MSLP west of SWWA and a southerly 850-hPa wind anomaly over SWWA in the ensemble mean of Factual compared to Counterfactual in 14 of the 30 days, with some anomalies over 2 hPa (Fig. ES29.2). POAMA shows a similar MSLP difference in Factual–Counterfactual for the month as *weather@home*, and an enhancement of the southerly wind anomaly at the south coast of SWWA (1.7 m s^{-1} in Counterfactual; 2.1 m s^{-1} in Factual, giving an $+0.4 \text{ m s}^{-1}$ anomaly; Fig. 29.2c). The wind signal over the wheat belt itself is weaker in POAMA than in *weather@home*; however, the MSLP signal west of SWWA is stronger.

Enhancement of MSLP west of SWWA was also found in the difference between the *weather@home* 1986–2015 Factual September climatology and the equivalent for Counterfactual, and between the POAMA 15-year September climatology of 2000–14 under current levels of carbon dioxide relative to the climatology with low levels (not shown). The consistency between the 2016 results and the climatologies suggests that the pattern is related to the change in the mean state of the atmosphere. The fact that POAMA shows a change similar to *weather@home* suggests that the changes in global carbon dioxide levels are of most importance in driving this signature, rather than ozone or aerosol changes (POAMA accounts only for changes in greenhouse gases; *weather@home* accounts for all forcings).

The blocking index was higher than average near SWWA on many days in September 2016, with seven blocked days detected within 60° – 140° E (Fig. 29.2d). Blocking was typically positive to the west of SWWA on the day of or prior to frosts (Fig. 29.2d). On 24 days during the month, there were significantly more blocking days detected in Factual simulations than in Counterfactual somewhere in the sector (stippled red regions in Fig. 29.2e), with only five days where there were significantly fewer (stippled blue). For example, on 25 September 2016 the mean detections at 140° E in Counterfactual is 0.03 detections day^{-1} , and this was enhanced by up to 0.04 detections day^{-1} in Factual. We don't expect the modeled timing of blocks to be precisely in phase with observations, so the exact timing of these differences is not the focus, but the *weather@home* results indicate a greater detection of blocked days on average across the region throughout.

weather@home showed warmer daily minimum temperatures and fewer frost risk days in the Factual simulations compared to the Counterfactual simulations (significant at the 5% level), suggesting

that the frost risk was lower due to human influence (Fig. ES29.3). Using a FAR analysis, experiencing 13 frost nights at a site in the wheat belt was in fact 45% less likely in Factual compared to Counterfactual. POAMA simulations also showed lower numbers of frost-risk days in Factual compared to Counterfactual (not shown). If the models simulated all the relevant processes regarding daily T_{min} with sufficient fidelity, then these results suggest that the circulation influence due to human influence did not fully offset the effect from a warmer mean temperature, so the net human influence was for fewer frosts. However, it is also likely that the models did not simulate all the dynamics required to produce frost nights, so the forced circulation difference may not have been expressed correctly in daily T_{min} . For example, the coarse resolution of the model may prevent the simulation of relevant mesoscale meteorological processes, and indeed the frequency in the Factual is lower than in the observed (Figs. 29.1a and ES29.3b).

Conclusion. Differences in MSLP, winds, and blocking between Factual and Counterfactual simulations from two modeling systems suggest that the circulation pattern associated with cold outbreaks was enhanced by human influence over southwest Western Australia in September 2016. However, the results also suggest warmer temperatures may have offset or countered this effect of the circulation driver on the overall frost risk for the month. Further work is needed to support this preliminary finding, including an assessment of the simulation of the circulation features and of minimum temperatures.

ACKNOWLEDGMENTS. This work was supported by the National Environmental Science Program Earth System and Climate Change hub (NESP ESCC). Many thanks to Eun-Pa Lim from the Bureau of Meteorology for providing POAMA outputs, Ian Foster from the Department of Agriculture, ERA-Interim, and *weather@home*.

REFERENCES

- Ashcroft, L., A. Pezza, and I. Simmonds, 2009: Cold events over Southern Australia: Synoptic climatology and hemispheric structure. *J. Climate*, **22**, 6679–6698, doi:10.1175/2009JCLI2997.1.
- BOM and CSIRO, 2016: State of the Climate 2016. Bureau of Meteorology and CSIRO, 22 pp. [Available online at www.bom.gov.au/state-of-the-climate/State-of-the-Climate-2016.pdf.]
- Cohen, J., and Coauthors, 2014: Recent Arctic amplification and extreme mid-latitude weather. *Nat. Geoscience*, **7**, 627–637, doi:10.1038/ngeo2234.
- Crimp, S. J., D. Gobbett, P. Kokic, U. Nidumolu, M. Howden, and N. Nicholls, 2016: Recent seasonal and long-term changes in southern Australian frost occurrence. *Climatic Change*, **139**, 115–128, doi.org/10.1007/s10584-016-1763-5.
- Dee, D. P., and Coauthors, 2011: The ERA-Interim reanalysis: configuration and performance of the data assimilation system. *Quart. J. Roy. Meteor. Soc.*, **137**, 553–597, doi:10.1002/qj.828.
- Gillett, N. P., J. C. Fyfe, and D. E. Parker, 2013: Attribution of observed sea level pressure trends to greenhouse gas, aerosol, and ozone changes. *Geophys. Res. Lett.*, **40**, 2302–2306, doi:10.1002/grl.50500.
- GIWA, 2016: October crop report [2016]. Grain Industry Association of Western Australia, 5 pp. [Available online at www.giwa.org.au/_literature_220446/GIWA_Crop_Report_-_October_2016.]
- Grose, M. R., J. S. Risbey, M. T. Black, and D. J. Karoly, 2015: Attribution of exceptional mean sea level pressure anomalies south of Australia in August 2014 [in “Explaining Extreme Events of 2014 from a Climate Perspective”]. *Bull. Amer. Meteor. Soc.*, **96** (12), S158–S162, doi:10.1175/BAMS-D-15-00116.1.
- , —, A. F. Moise, S. Osbrough, C. Heady, L. Wilson, and T. Erwin, 2017: Constraints on Southern Australian rainfall change based on atmospheric circulation in CMIP5 simulations. *J. Climate*, **30**, 225–242, doi:10.1175/JCLI-D-16-0142.1.
- Guillod, B. P., and Coauthors, 2017: weather@home 2: Validation of an improved global–regional climate modelling system. *Geosci. Model Dev.*, **10**, 1849–1872, doi:10.5194/gmd-10-1849-2017.
- Hope, P., E.-P. Lim, G. Wang, H. H. Hendon, and J. M. Arblaster, 2016: What caused the record-breaking heat across Australia in October 2015? [in “Explaining Extreme Events of 2015 from a Climate Perspective”]. *Bull. Amer. Meteor. Soc.*, **97** (12), S122–S126, doi:10.1175/BAMS-D-16-0142.1.
- , —, H. H. Hendon, and G. Wang, 2018: The effect of increasing CO₂ on the extreme September 2016 rainfall across south eastern Australia [in “Explaining Extreme Events of 2016 from a Climate Perspective”]. *Bull. Amer. Meteor. Soc.*, **99** (1), S133–S138, doi: 10.1175/BAMS-D-17-0094.1.
- Jones, D. A., W. Wang, and R. Fawcett, 2009: High-quality spatial climate data-sets for Australia. *Aust. Meteor. Oceanogr. J.*, **58**, 233–248.
- Mann, M. E., S. Rahmstorf, K. Kornhuber, B. A. Steinman, S. K. Miller, and D. Coumou, 2017: Influence of anthropogenic climate change on planetary wave resonance and extreme weather events. *Sci. Rep.*, **7**, 45242, doi:10.1038/srep45242.
- Marshall, A. G., D. A. Hudson, H. H. Hendon, M. J. Pook, O. Alves, and M. C. Wheeler, 2014: Simulation and prediction of blocking in the Australian region and its influence on intra-seasonal rainfall in POAMA-2. *Climate Dyn.*, **42**, 3271–3288, doi:10.1007/s00382-013-1974-7.
- Mitchell, D., and Coauthors, 2017: Assessing mid-latitude dynamics in extreme event attribution systems. *Climate Dyn.*, **48**, 3889–3901, doi:10.1007/s00382-016-3308-z.
- Pook, M. J., J. S. Risbey, and P. C. McIntosh, 2011: The synoptic climatology of cool-season rainfall in the central wheatbelt of Western Australia. *Mon. Wea. Rev.*, **140**, 28–43, doi:10.1175/MWR-D-11-00048.1.
- Taylor, K. E., R. J. Stouffer, and G. A. Meehl, 2012: An overview of CMIP5 and the experiment design. *Bull. Amer. Meteor. Soc.*, **93**, 485–498, doi:10.1175/BAMS-D-00094.1.
- Tibaldi, S. and F. Molteni, 1990: On the operational predictability of blocking. *Tellus A*, **42**, 343–365, doi:10.1034/j.1600-0870.1990.t01-2-00003.x
- Wang, G., P. K. Hope, E.-P. Lim, H. H. Hendon, and J. M. Arblaster, 2016: Three methods for the attribution of extreme weather and climate events. [Australia] Bureau of Meteorology Research Rep. 018, 32 pp. [Available online at www.bom.gov.au/research/publications/researchreports/BRR-018.pdf.]
- Zhang, J., W. Tian, M. P. Chipperfield, F. Xie, and J. Huang, 2016: Persistent shift of the Arctic polar vortex towards the Eurasian continent in recent decades. *Nat. Climate Change*, **6**, 1094–1099, doi:10.1038/nclimate3136.

Table I.I. SUMMARY of RESULTS

ANTHROPOGENIC INFLUENCE ON EVENT			
	INCREASE	DECREASE	NOT FOUND OR UNCERTAIN
Heat	Ch. 3: Global Ch. 7: Arctic Ch. 15: France Ch. 19: Asia		
Cold		Ch. 23: China Ch. 24: China	
Heat & Dryness	Ch. 25: Thailand		
Marine Heat	Ch. 4: Central Equatorial Pacific Ch. 5: Central Equatorial Pacific Ch. 6: Pacific Northwest Ch. 8: North Pacific Ocean/Alaska Ch. 9: North Pacific Ocean/Alaska Ch. 9: Australia		Ch. 4: Eastern Equatorial Pacific
Heavy Precipitation	Ch. 20: South China Ch. 21: China (Wuhan) Ch. 22: China (Yangtze River)		Ch. 10: California (failed rains) Ch. 26: Australia Ch. 27: Australia
Frost	Ch. 29: Australia		
Winter Storm			Ch. 11: Mid-Atlantic U.S. Storm "Jonas"
Drought	Ch. 17: Southern Africa Ch. 18: Southern Africa		Ch. 13: Brazil
Atmospheric Circulation			Ch. 15: Europe
Stagnant Air			Ch. 14: Western Europe
Wildfires	Ch. 12: Canada & Australia (Vapor Pressure Deficits)		
Coral Bleaching	Ch. 5: Central Equatorial Pacific Ch. 28: Great Barrier Reef		
Ecosystem Function		Ch. 5: Central Equatorial Pacific (Chl- α and primary production, sea bird abundance, reef fish abundance) Ch. 18: Southern Africa (Crop Yields)	
El Niño	Ch. 18: Southern Africa		Ch. 4: Equatorial Pacific (Amplitude)
TOTAL	18	3	9

METHOD USED		Total Events
Heat	Ch. 3: CMIP5 multimodel coupled model assessment with piCont, historicalNat, and historical forcings Ch. 7: CMIP5 multimodel coupled model assessment with piCont, historicalNat, and historical forcings Ch. 15: Flow analogues conditional on circulation types Ch. 19: MIROC-AGCM atmosphere only model conditioned on SST patterns	
Cold	Ch. 23: HadGEM3-A (GA6) atmosphere only model conditioned on SST and SIC for 2016 and data fitted to GEV distribution Ch. 24: CMIP5 multimodel coupled model assessment	
Heat & Dryness	Ch. 25: HadGEM3-A N216 Atmosphere only model conditioned on SST patterns	
Marine Heat	Ch. 4: SST observations; SGS and GEV distributions; modeling with LIM and CGCMs (NCAR CESM-LE and GFDL FLOR-FA) Ch. 5: Observational extrapolation (OISST, HadISST, ERSST v4) Ch. 6: Observational extrapolation; CMIP5 multimodel coupled model assessment Ch. 8: Observational extrapolation; CMIP5 multimodel coupled model assessment Ch. 9: Observational extrapolation; CMIP5 multimodel coupled model assessment	
Heavy Precipitation	Ch. 10: CAM5 AMIP atmosphere only model conditioned on SST patterns and CESM1 CMIP single coupled model assessment Ch. 20: Observational extrapolation; CMIP5 and CESM multimodel coupled model assessment; auto-regressive models Ch. 21: Observational extrapolation; HadGEM3-A atmosphere only model conditioned on SST patterns; CMIP5 multimodel coupled model assessment with ROF Ch. 22: Observational extrapolation, CMIP5 multimodel coupled model assessment Ch. 26: BoM seasonal forecast attribution system and seasonal forecasts Ch. 27: CMIP5 multimodel coupled model assessment	
Frost	Ch. 29: <i>weather@home</i> multimodel atmosphere only models conditioned on SST patterns; BoM seasonal forecast attribution system	
Winter Storm	Ch. 11: ECHAM5 atmosphere only model conditioned on SST patterns	
Drought	Ch. 13: Observational extrapolation; <i>weather@home</i> multimodel atmosphere only models conditioned on SST patterns; HadGEM3-A and CMIP5 multimodel coupled model assessment; hydrological modeling Ch. 17: Observational extrapolation; CMIP5 multimodel coupled model assessment; VIC land surface hydrological model, optimal fingerprint method Ch. 18: Observational extrapolation; <i>weather@home</i> multimodel atmosphere only models conditioned on SSTs, CMIP5 multimodel coupled model assessment	
Atmospheric Circulation	Ch. 15: Flow analogues distances analysis conditioned on circulation types	
Stagnant Air	Ch. 14: Observational extrapolation; Multimodel atmosphere only models conditioned on SST patterns including: HadGEM3-A model; EURO-CORDEX ensemble; EC-EARTH+RACMO ensemble	
Wildfires	Ch. 12: HadAM3 atmosphere only model conditioned on SSTs and SIC for 2015/16	
Coral Bleaching	Ch. 5: Observations from NOAA Pacific Reef Assessment and Monitoring Program surveys Ch. 28: CMIP5 multimodel coupled model assessment; Observations of climatic and environmental conditions (NASA GES DISC, HadCRUT4, NOAA OISSTV2)	
Ecosystem Function	Ch. 5: Observations of reef fish from NOAA Pacific Reef Assessment and Monitoring Program surveys; visual observations of seabirds from USFWS surveys. Ch. 18: Empirical yield/rainfall model	
El Niño	Ch. 4: SST observations; SGS and GEV distributions; modeling with LIM and CGCMs (NCAR CESM-LE and GFDL FLOR-FA) Ch. 18: Observational extrapolation; <i>weather@home</i> multimodel atmosphere only models conditioned on SSTs, CMIP5 multimodel coupled model assessment	